# THE VALUE OF BOREHOLE -TO-SURFACE INFORMATION IN NEAR-SURFACE CROSSWELL SEISMIC TOMOGRAPHY

*Geoff J. M. Moret, The Pennsylvania State University, University Park, PA*
*Michael D. Knoll, CGISS, Boise State University, Boise, ID*

## Abstract

Detailed information about the spatial distribution of subsurface properties is important in many fields. One method that can image the seismic velocity structure of the shallow subsurface is crosswell seismic tomography. By including rays traveling from the boreholes to the surface, the angular coverage of crosswell tomograms can be significantly improved. We investigated the effects of these borehole-to-surface rays on synthetic and field data. The tests on synthetic data showed that including borehole-to-surface information did not significantly change the tomogram's resolution. Tomographic inversion of a field data set collected at the Boise Hydrogeophysical Research Site, however, showed that including borehole-to-surface information improves a tomogram's ability to image layer boundaries, and improves the velocity estimates for slow layers. The tomogram generated using the crosswell and borehole-to-surface information is consistent with the previously interpreted hydrostratigraphic units at the site.

## Introduction

Detailed information about subsurface structure and material properties is needed for many earth science applications. Geophysical methods can be a cost-effective and minimally-invasive way to obtain this information. One such method is crosswell seismic traveltime tomography. Crosswell seismic traveltime tomography involves recording the traveltimes between many source and receiver positions in different wells, and then inverting these data to produce a velocity model consistent with these observations. This velocity model can be used for engineering purposes (Jessop et al, 1992), waste site characterization (Moyle et al., 1994), hydrogeological property characterization (Hyndman et al., 1994; Peterson et al., 1999), or any other application where a knowledge of subsurface seismic properties or architecture is needed. Crosswell seismic tomography can produce useful images in situations where surface seismic reflection cannot (e.g. Liberty et al., 1999; Musil et al., 2002).

The images produced with crosswell seismic traveltime tomography are not always accurate and reliable, however. The resolution and certainty of the tomograms are controlled by the signal wavelength, data noise, regularization scheme, forward model, and source and receiver geometry. In some cases, the resolution of tomographic images is limited by the angular coverage of sources and receivers (Rector and Washbourne, 1994). The angular coverage of crosswell tomography is inherently limited by the acquisition geometry.

Rays traveling from the borehole to the surface (offset RVSP rays) can be included in tomographic reconstructions to improve the angular coverage (Aldridge and

Oldenburg, 1992; Curtis, 1998). This is not often done in deep crosswell surveys, but it is feasible for many environmental and engineering surveys. The additional data can be collected easily, and the resulting tomograms should in general have more accurate velocities and better resolution of subsurface structure.

In this paper, we demonstrate the value of including borehole-to-surface information in shallow seismic tomography. First we use a synthetic example to investigate the effect of high angle rays on tomographic reconstructions. Then we invert crosswell and borehole-to-surface traveltimes from a field data set collected at the Boise Hydrogeophysical Research Site to demonstrate the technique in a real world situation.

## Synthetic Example

To investigate the value of including borehole-to-surface rays in seismic traveltime inversion, we conducted a synthetic modeling study. The earth model we used for the modeling (Figure 1) is meant to simulate an unconfined aquifer with a velocity of 330 m/s above the water table and several different units with velocities between 2100 and 2500 m/s below the water table. We simulated crosswell and borehole-to-surface traveltimes through the velocity model, and constructed tomograms with and without the borehole-to-surface traveltimes.

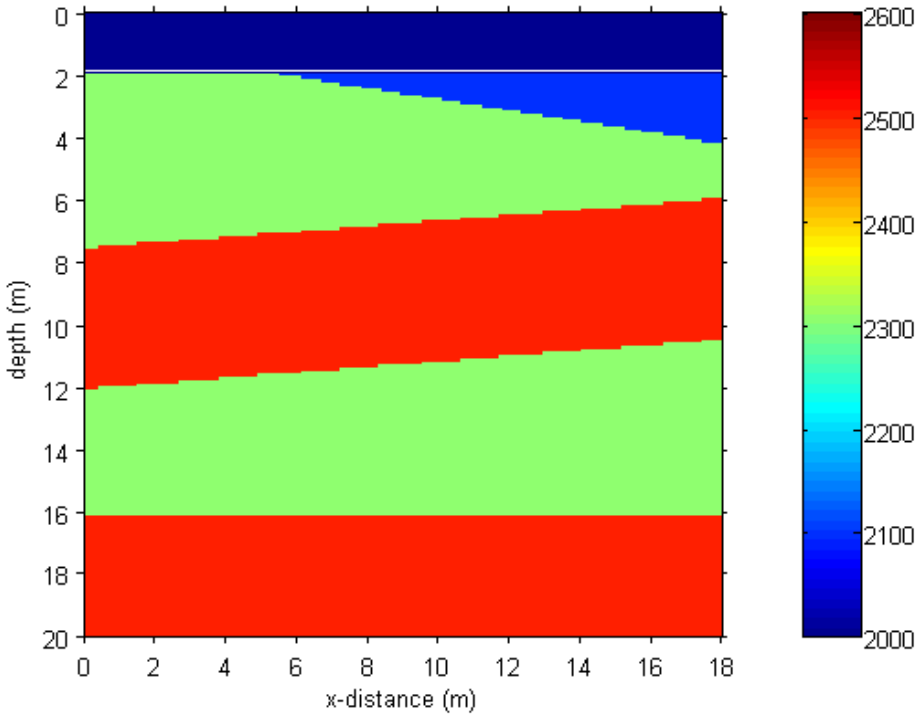


**Figure 1:** Velocity model used to generate synthetic data. The velocity is 330 m/s above 1.95 m depth.

We modeled the traveltimes using a finite difference approximation to the eikonal equation (Vidale, 1988; Aldridge and Oldenburg, 1993). This method includes ray-bending at velocity contrasts. The shot and receiver locations were identical to those of

the field experiment described in the next section. The accuracy of the forward modeling routine is limited by the grid size (Aldridge and Oldenburg, 1993). We used a fine grid (0.1 m), to ensure the accuracy of the modeled traveltimes. We added Gaussian noise with a standard deviation of 0.06 ms to traveltimes to simulate picking error.

We inverted the synthetic traveltimes using the program Pronto (Aldridge and Oldenburg, 1993), an iterative, curved-ray routine that can incorporate various types of model constraints. The constraint equations we chose to use minimized the vertical and horizontal first derivatives of the velocity field, and the difference between the velocity field and a reference model. We used a two-layer reference model with a velocity of 300 m/s above the water table and 2400 m/s below the water table. The horizontal, vertical, and reference model constraints were weighted with values of 4000, 400, and 100 respectively. We chose these values by comparing the inversion results (with and without the borehole-to-surface information) for different weights, and selecting a set of weights that produced velocity models similar to the true velocity model.

Figure 2 shows the tomogram produced by inverting the synthetic crosswell data without borehole-to-surface information. The positions of the velocity zones are imaged well. The actual velocities of these zones, however, are not estimated correctly, as the velocities of the 2500 m/s zones are slightly too low and the velocities of the 2300 m/s zones are slightly too high. These velocity errors are a result of the regularization. The small 2100 m/s zone in the upper right of the velocity model is not resolved.

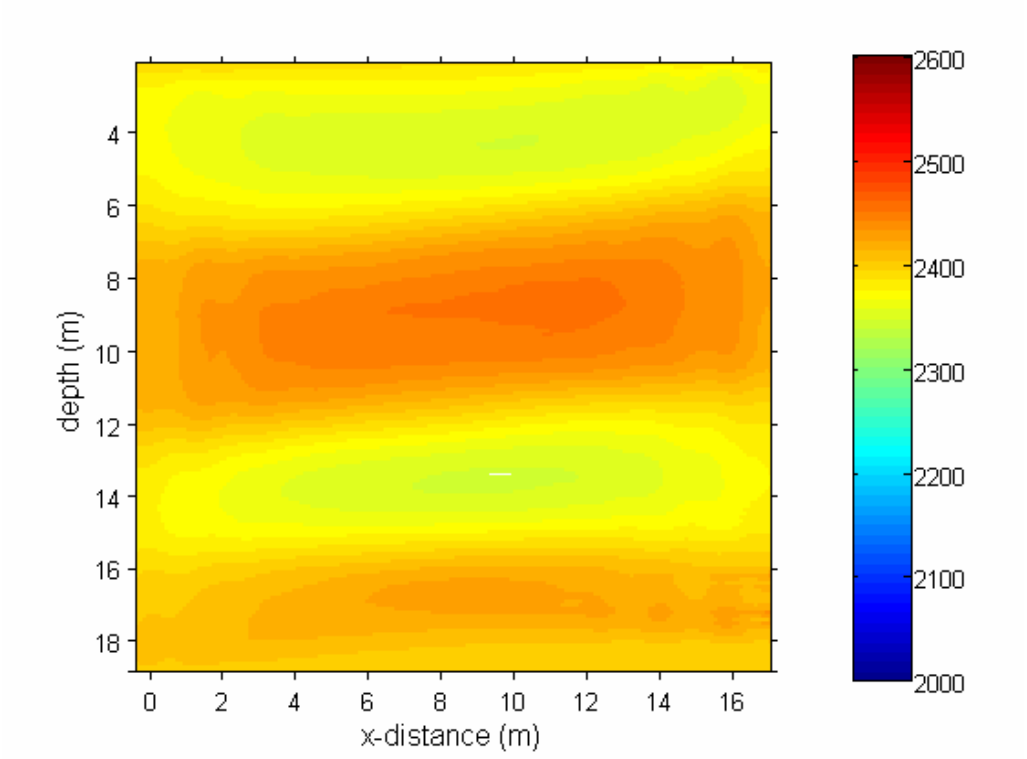


**Figure 2:** Tomogram generated using synthetic crosswell data.

Figure 3 shows the tomogram produced by inverting the synthetic crosswell and borehole-to-surface data. The zone boundaries are located with the same accuracy as the exclusively crosswell tomogram. The 2100 m/s zone at the top right is imaged in this tomogram, but the resolution of this feature is so poor that it could be interpreted as an

artifact if the true model were unknown. The vertical streaking near the wells is an artifact caused by the inclusion of borehole-to-surface information in the tomographic inversion. These synthetic results do not indicate that there is a significant advantage in including borehole-to-surface information in crosswell tomography at a site with this sort of velocity structure apart from a possible slight improvement in the resolution of heterogeneities near the top of the tomogram.

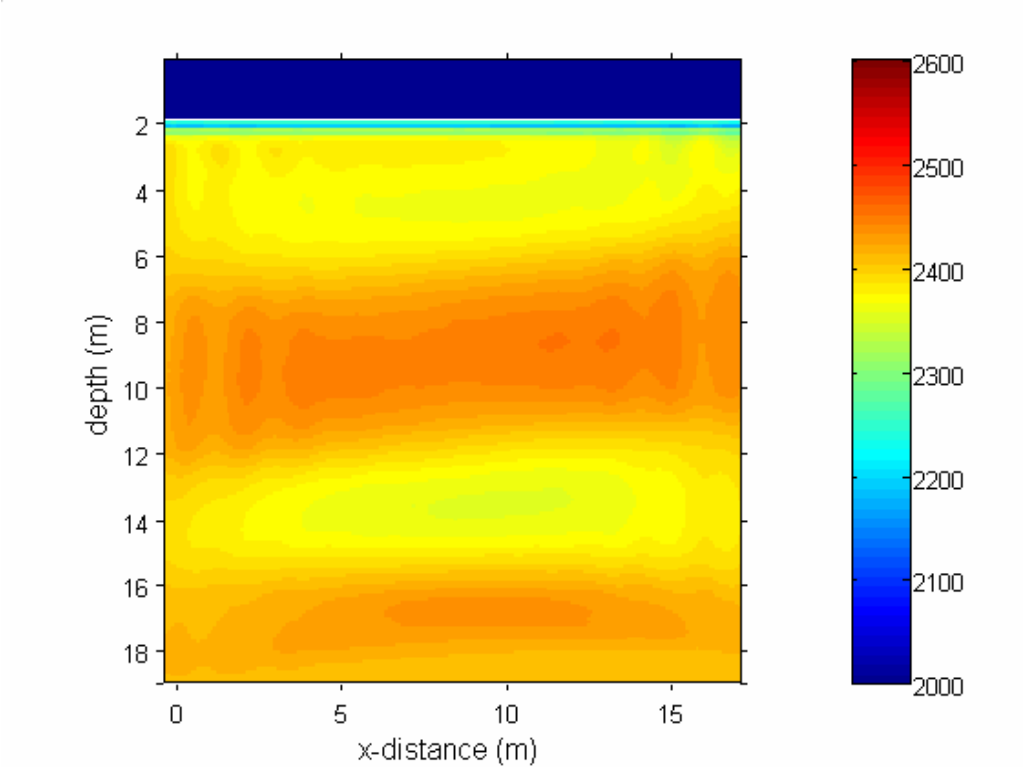


**Figure 3:** Tomogram generated using synthetic crosswell and borehole-to-surface data. The velocity above 1.95 m is within 5 m/s of 330 m/s.

## Field Example

To test the value of borehole-to-surface information in a real world setting, we conducted a field test at the Boise Hydrogeophysical Research Site (BHRS). The BHRS is a research wellfield in a shallow, unconsolidated aquifer near Boise, ID (Figure 4). The BHRS was designed to support the development and testing of geophysical methods to characterize the shallow subsurface (Barrash and Knoll, 1998) and in particular to develop integrated hydrogeophysical methods to study flow and transport behaviour. The water table in this aquifer varies with the river level, but is often roughly 2 m below the surface. The BHRS consists of an approximately 20 m thick layer of coarse alluvial sediments underlain by a clay aquitard. The aquifer sediments are chiefly cobble-dominated deposits, with some sand lenses.

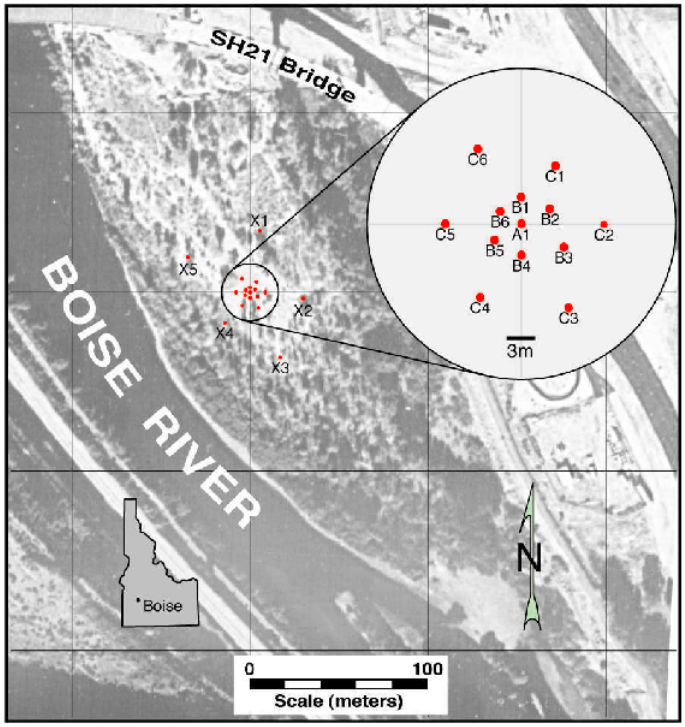


**Figure 4:** Aerial photograph, map, and well field layout of the BHRS. Figure courtesy of Ed Reboulet.

As shown in Figure 4, 13 wells have been emplaced in a pattern meant to thoroughly characterize a control volume of about 20 m diameter and 20 m depth with well A1 in the center. The other 12 wells in the central area consist of an inner ring roughly 3 m from A1 (wells B1-B6), and an outer ring between 7 and 10 m from A1 (wells C1-C6). There is also a set of boundary wells roughly 20 to 40 m from A1 (wells X1-X5). The wells were drilled to a depth of ~20 m, and cased with 4" PVC well screen. Special care was taken during drilling and well completion to minimize the annular space and disturbed zone surrounding the well screen (Barrash and Knoll, 1998). The finished well site is suitable for surface-to-surface, surface-to-well, and crosswell geophysics, as well as a wide variety of hydrologic tests (Barrash et al., 1999; Clement et al., 1999).

Using GPR reflection (Perreti et al., 1999), grain size analysis (Reboulet and Barrash, 2000) and neutron log-based porosity estimates, Barrash and Clemo (2002) identified five major sedimentary units at the site (Figure 5). Units 1 and 3 are low porosity (mean porosities of 0.18 and 0.17, respectively) cobble and sand deposits. Units 2 and 4 are higher porosity (mean porosities of 0.24 and 0.23, respectively) cobble and sand deposits, with more variation in porosity values than units 1 and 3. Unit 5 is a high porosity channel sand (mean porosity of 0.43) that overlies the southern part of the BHRS.

We collected seismic tomography data between wells C1 and C4 at the BHRS on June 21 and 22, 2002, using a borehole sparker (British Geological Survey control unit, Sub Terra Surveys sonde), down-hole hydrophone string, and surface geophones. The sparker is a rubber-walled cell full of salt water containing a spark gap. When a high voltage (approximately 4 kV) is discharged across the spark gap, the ionization of a small

amount of salt water due to the electric current creates an acoustic disturbance. The seismic data recorded using the sparker at the BHRS have a peak frequency of roughly1200 Hz. The coupling of the sparker with the surrounding formation has a large effect on data quality. In the saturated zone, the borehole fluid transmits the P-wave energy. In dry holes, however the coupling between the sparker and the formation is not strong unless a special clamped sparker is used. For this survey, we only fired the sparker below the water table.

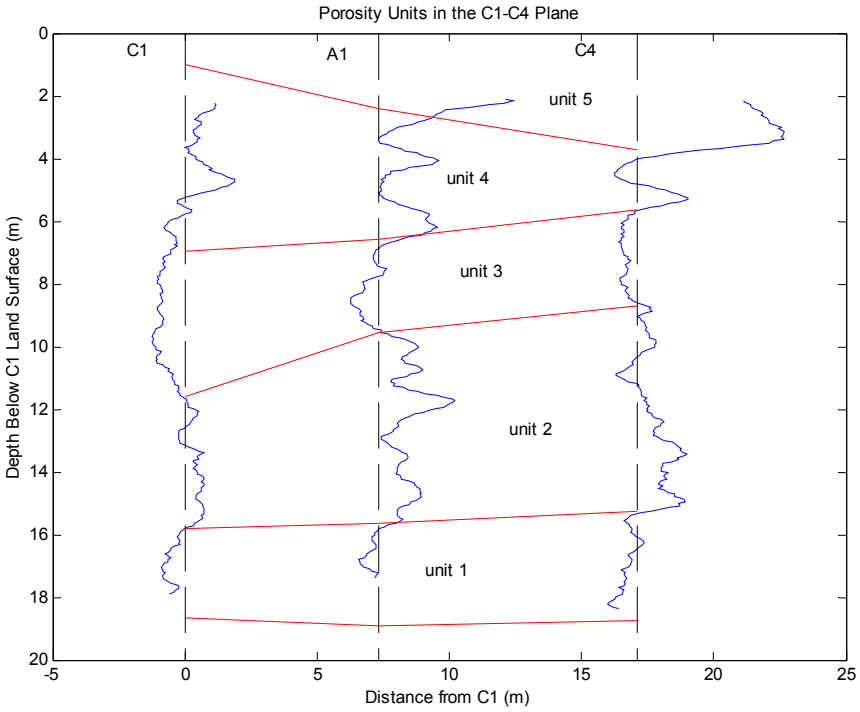


**Figure 5:** Interpreted porosity units in the C1-C4 plane. The vertical dashed lines are the well locations, and also represent 0.20 on the porosity logs. The depth of the unit 4-unit 5 boundary in well C1 is arbitrary because unit 5 is not present in the C1 porosity log.

A borehole hydrophone string was used to collect the crosswell data. The string consists of 37 hydrophones spaced 0.5 m apart. The horizontal positions of the hydrophones were determined using borehole deviation logs. The data were recorded on a 24-bit engineering seismograph (Geometrics Strataview NZ-48) with a 0.0625 ms sample interval.

We had initially planned to collect surface-to-borehole information using a hammer source and the hydrophone string. These data, however, had a lower frequency content than the sparker data. In addition, timing errors were introduced by near-source compaction with repeated hammer blows. We also attempted to collect borehole-to-surface data using a piezoelectric source, but, due to high attenuation in the vadose zone, the recorded signal was too weak unless more than 200 stacks were used. We chose instead to collect borehole-to-surface information by firing the sparker into vertical-component geophones. One benefit of this approach is that much of the data can be collected at the same time as the crosswell data. We buried the geophones approximately 15 cm deep to reduce their sensitivity to surface noise. The x, y, and z positions of the

geophones were determined using a survey tape and measuring rod. This survey was tied to well locations surveyed using GPS and a total station surveying instrument.

The sparker was fired in well C1 at 0.1 m intervals from just below the water table (2.4 m below the surface) to the bottom of the well (18.8 m below the surface). This series of shots was repeated five times, and each time the hydrophone string in well C4 was raised 0.1 m, for an effective borehole receiver spacing of 0.1 m. The geophones were located every 1 m along the surface between the two wells. After the crosswell data had been acquired, the sparker was moved to C4 to collect borehole-to-surface rays into the geophones from the other side of the image plane. Approximately 28,000 traces were collected for this experiment. The first breaks of the data were manually picked using ProMAX, a commercial seismic processing package.

The tomography was carried out using the procedure described in the synthetic example section. The constraint weights chosen for the synthetic data were used to invert the field data. This is appropriate because the source and receiver positions and velocity model in the synthetic modeling were chosen to be similar to the field experiment. The reference model (330 m/s above 1.95 m depth, 2400 m/s below) was produced using the results of a refraction survey and water level measurements in the wells at the time of data collection. The tomogram produced with only crosswell data are shown in Figure 6. The tomogram produced with crosswell and borehole-to-surface data are shown in Figure 7.

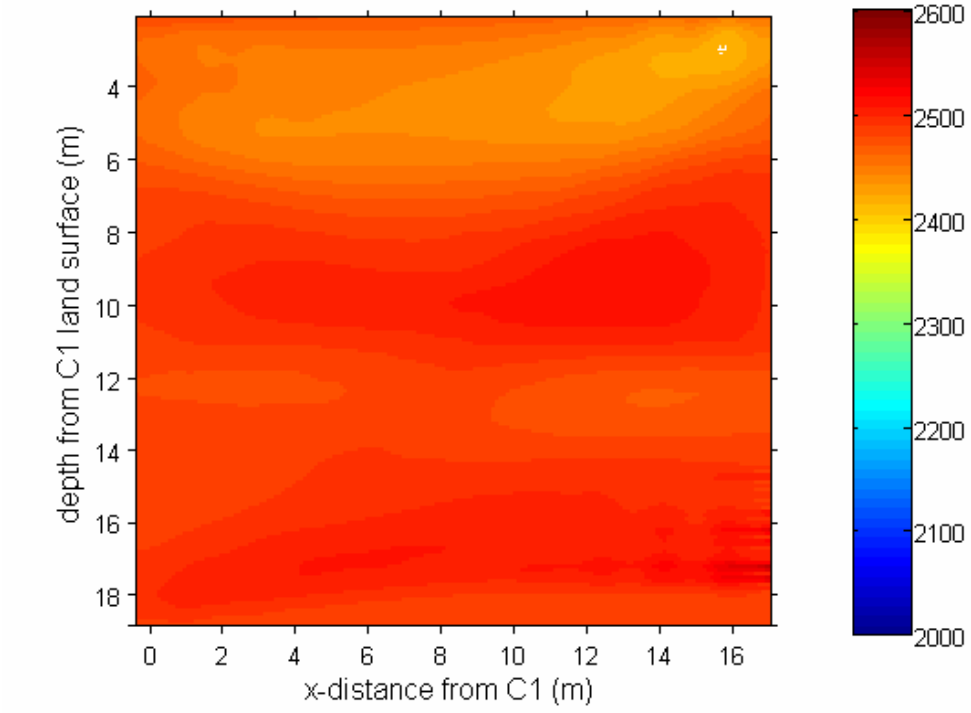


**Figure 6:** Tomogram generated using crosswell data collected at the BHRS.

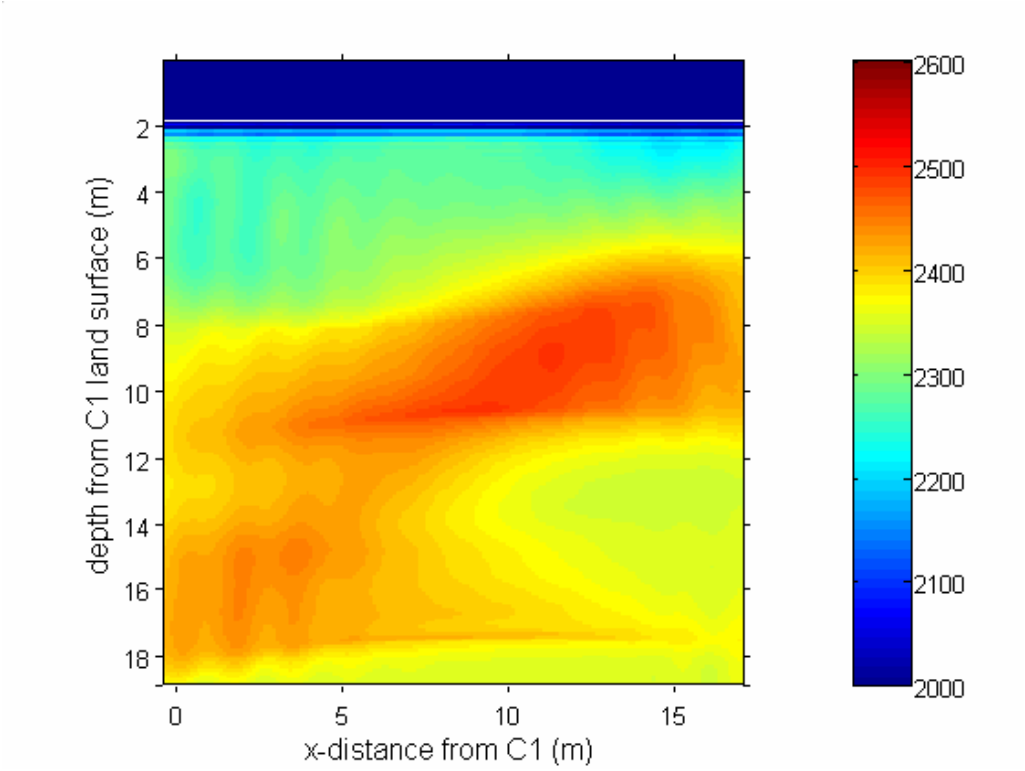


**Figure 7:** Tomogram generated using crosswell and borehole-to-surface data collected at the BHRS. The velocity above 1.95 m is within 5 m/s of 330 m/s.

## Discussion

Both Figures 6 and 7 show layered systems. The slow layers (units 2 and 4) in the strictly-crosswell tomogram, however, have higher velocities than the slow layers in the tomogram with borehole-to-surface information included (about 2300-2400 m/s vs. >2400 m/s). This difference in slow zone velocities was not seen in the synthetic data. Crosswell raypaths refract to travel through the fast zones, so the slow layer velocities are poorly constrained. In the synthetic example, where the traveltimes were modeled using ray theory, which assumes the seismic energy has zero wavelength, enough rays traveled through the slow zones to obtain a good estimate of their velocities. In the field example, however, where the seismic energy has a wavelength near the scale of the structures being imaged (approximately 2 m, if the frequency is 1200 Hz and the velocity is 2400 m/s), the support volume of the measurements can be large (e.g. Williamson and Worthington, 1993; Schuster, 1996). Thus, the rays that traveled solely through the slow zones in the synthetic example are affected by the surrounding fast zones in the field example. The borehole-to-surface rays travel generally perpendicular to the zone boundaries, sampling each layer individually, so the borehole-to-surface information in the tomographic inversion makes the result more sensitive to slow zone velocities.

Larger support volumes may also be responsible for the improved resolution of zone boundaries in the borehole-to-surface information included tomogram. The result with the borehole-to-surface rays included (Figure 7), images a sloping contact between units 3 and 4 as seen in the neutron-log based units (Figure 6), while the crosswell-only tomogram in Figure 6 shows the contact as nearly horizontal. The synthetic data are able

to resolve the position of a similar contact with only crosswell data (Figure 2). The resolution of the field data is considerably poorer due to the larger support volumes, however, so the additional angular coverage provided by the borehole-to-surface information is required to image the exact geometry of the boundary.

The ability of crosswell seismic tomography with borehole-to-surface information to resolve subsurface structure can be assessed by comparing the tomogram of Figure 8 with the neutron log-based units of Figure 5. The small piece of unit 5 that extends below the vadose zone near well C4 cannot be imaged. The agreement between the two figures is excellent for the boundaries between units 3 and 4 and units 2 and 3. The boundary between units 1 and 2 is only a few meters above the bottom of the tomogram, and therefore cannot be reliably imaged. These results show that seismic tomography with borehole-to-surface information included can be a useful tool for delineating subsurface structure at sites such as the BHRS.

## Conclusions

Angular coverage can be an important factor in determining the resolution of crosswell tomograms. Because most engineering and environmental tomography surveys are collected very near the surface, borehole-to-surface data can be acquired with little extra fieldwork. Including the additional traveltimes in the tomographic inversion is trivial, as most algorithms do not restrict the locations of sources and receivers. The field example presented here shows that including borehole-to-surface rays in crosswell tomography can improve the results in two ways: by more accurately imaging subsurface structure, and by improving the estimated velocities, particularly in slow zones.

Interesting questions are raised by the lack of improvement in the synthetic tomography results with the inclusion of borehole-to-surface information. We have explained this result by attributing the large improvement in the field data set to the larger support volume of the filed measurements. This theory could be tested by using a more realistic forward model (one with a non-zero support volume) to generate synthetic data. If the synthetic tomograms generated using this new synthetic data had resolution similar to the tomograms produced using field data then it would indicate that a tomography routine that went beyond ray theory (e.g. Vasco et al., 1995) would be more appropriate than the routine used here.

More work remains to be done on incorporating borehole-to-surface information into crosswell tomography. Including surface-to-surface data (i.e. a refraction survey) or using clamped sparkers and geophones above the water table could improve the vadose zone characterization, but care would have to be taken in combining data from seismic sources with different spectra and different triggering. A less ad hoc way of determining the constraint weights could also improve the result. Careful analysis of the dependence of the tomograms on the reference model is needed. Ideally, angular coverage could be further improved by drilling horizontal wells at depth. In the absence of this, however, the traveltimes of reflections off of reflectors of known depth could be used (Tronicke et al., 2001). Even without these refinements, however, this paper has demonstrated that including borehole-to-surface information in crosswell seismic tomography can improve our ability to image subsurface structure.

## Acknowledgements

The authors would like to thank David Aldridge for the use of his code, Bill Clement for several useful discussions, and Mike Procsal, Marc Buursink, and Greg Oldenberger for field help. This project was funded by Environmental Protection Agency (EPA) grant X-970085-01-0, and Army Research Office grants DAAH-4-96-1-0318 and DAAG55-98-1-0277.

## References

1. Aldridge, D.F., and Oldenburg, D.W., 1992, Two dimensional tomographic inversion with finite-difference traveltimes: Proc., Canadian Society of Exploration Geophysics National Convention, May 5-8, Calgary, Alberta, 76-77.
2. Aldridge, D.F., and Oldenburg, D.W., 1993, Two-dimensional tomographic inversion with finite-difference traveltimes: Journal of Seismic Exploration, **2**, 257-274.
3. Barrash, W. and Clemo, T., 2002, Hierarchical geostatistics and multifacies systems: Boise Hydrogeophysical Research Site, Boise, Idaho, Water Resources Research , **38**, 1196, doi:10.1029/2001WR001259, 2002.
4. Barrash, W., Clemo, T., and Knoll, M.D., 1999, Boise Hydrogeophysical Research Site: Objectives, design, initial geostatistical results: Proc., SAGEEP, Env. Eng. Geophys. Soc., 389-398.
5. Barrash, W., and Knoll, M.D., 1998, Design of research wellfield for calibrating geophysical methods against hydrologic parameters: Proc., Conference on Hazardous Waste Research, Great Plains/Rocky Mountains Hazardous Substance Research Center, 269-318.
6. Clement, W.P., Knoll, M.D., Liberty, L.M., Donaldson, P.R., Michaels, P., Barrash, W., and Pelton, J.R., 1999, Geophysical surveys across the Boise Hydrogeophysical Research Site to determine geophysical parameters of a shallow, alluvial aquifer: Proc., SAGEEP, Env. Eng. Geophys. Soc., 399-408.
7. Curtis, A., 1998, Optimal cross-borehole tomographic geometries: SEG Annual Meeting Expanded Abstracts, New Orleans, LA, Sept 13-18, 797-800.
8. Hyndman, D.W., Harris, J.M., and Gorelick, S.M., 1994, Coupled seismic and tracer test inversion for aquifer property characterization: Water Resources Research, **30**, 1965-1977.
9. Jessop, J.A., Friedel, M.J., Jackson, M.J., and Tweeton, D.R., 1992, Fracture detection with seismic crosshole tomography for solution control in a stope: Proc., SAGEEP, Env. Eng. Geophys. Soc., 487-507.
10. Liberty, L.M., Clement, W.P., and Knoll, M.D., 1999, Surface and borehole seismic characterization of the Boise Hydrogeophysical Research Site: Proc., SAGEEP, Env. Eng. Geophys. Soc., 723-732.
11. Moyle, P.R., Fay, J.M., and Friedel, M.J., 1994, Integrated geophysical characterization f mine-waste sites in the Coeur D'Alene mining district, Idaho: Proc., SAGEEP, Env. Eng. Geophys. Soc., 857-868.

12. Musil, M., Maurer, H., Green, A., Horstmeyer, H., Nitsche, F., Vonder Muhll, D, and Springman, S., 2002, Shallow seismic surveying of an alpine rock glacier: Geophysics, **67**, 1701-1710.
13. Peretti, W., Knoll, M.D., Clement, W.P., and Barrash, W., 1999, 3-D GPR imaging of complex fluvial stratigraphy at the Boise Hydrogeophysical Research Site: Proc., SAGEEP, Env. Eng. Geophys. Soc., 555-564.
14. Peterson, J.E., 2001, Pre-inversion corrections and analysis of radar tomographic data: Journal of Environmental and Engineering Geophysics, **6**, 1-18.
15. Reboulet, E.C. and Barrash, W., 2000 Statistical analysis of grain-size distribution and porosity data from coarse braided-stream deposits at the Boise Hydrogeophysical Research Site (abs.): Geological Society of America Annual Meeting, November 13-16, 2000, Reno, NV, Abstracts with Programs, v. 32, no. 7, p. A410.
16. Rector, J.W., and Washbourne, J.K., 1994, Characterization of the resolution and uniqueness in crosswell direct-arrival traveltime tomography using the Fourier projection slice theorem: Geophysics, **59**, 1642-1649.
17. Schuster**,** G.T., 1996, Resolution limits for crosswell migration and traveltime tomography: Geophysical Journal International, **127**, 427-440.
18. Tronicke, J, Tweeton, D., Dietrich, P., and Appel, E., 2001, Improved crosshole radar tomography by using direct and reflected arrival times: Journal of Applied Geophysics, **47**, 97-105.
19. Vasco, D.W., Peterson, J.E., and Majer, E.L., 1995, Beyond ray tomography; wavepaths and Fresnel volumes: Geophysics, **60**, 1790-1804.
20. Vidale, J., 1988, Finite-difference calculation of travel times: Bulletin of the Seismological Society of America, **78**, 2062-2076.
21. Williamson, W.R., and Worthington, M.H., 1993, Resolution limits in ray tomography due to wave behavior: numerical experiments: Geophysics, **58**, 727-735.